

This article was downloaded by: [Biblioteka Główna Politechniki]

On: 03 May 2015, At: 23:19

Publisher: Taylor & Francis

Informa Ltd Registered in England and Wales Registered Number: 1072954 Registered office: Mortimer House, 37-41 Mortimer Street, London W1T 3JH, UK



## Journal of Thermal Stresses

Publication details, including instructions for authors and subscription information:

<http://www.tandfonline.com/loi/uths20>

### On a Contact Problem of Two-Layer Beams Coupled by Boundary Conditions in a Temperature Field

Anton V. Krysko<sup>a</sup>, Jan Awrejcewicz<sup>b</sup>, Igor E. Kutepov<sup>c</sup> & Vadim A. Krysko<sup>c</sup>

<sup>a</sup> Department of Applied Mathematics and Systems Analysis, Saratov State Technical University, Saratov, Russian Federation

<sup>b</sup> Department of Automation, Biomechanics and Mechatronics, Lodz University of Technology, Lodz and Department of Vehicles, Warsaw University of Technology, Warsaw, Poland

<sup>c</sup> Department of Mathematics and Modeling, Saratov State Technical University, Saratov, Russian Federation

Published online: 27 Apr 2015.



[Click for updates](#)

To cite this article: Anton V. Krysko, Jan Awrejcewicz, Igor E. Kutepov & Vadim A. Krysko (2015) On a Contact Problem of Two-Layer Beams Coupled by Boundary Conditions in a Temperature Field, Journal of Thermal Stresses, 38:5, 468-484, DOI: [10.1080/01495739.2015.1015848](https://doi.org/10.1080/01495739.2015.1015848)

To link to this article: <http://dx.doi.org/10.1080/01495739.2015.1015848>

PLEASE SCROLL DOWN FOR ARTICLE

Taylor & Francis makes every effort to ensure the accuracy of all the information (the "Content") contained in the publications on our platform. However, Taylor & Francis, our agents, and our licensors make no representations or warranties whatsoever as to the accuracy, completeness, or suitability for any purpose of the Content. Any opinions and views expressed in this publication are the opinions and views of the authors, and are not the views of or endorsed by Taylor & Francis. The accuracy of the Content should not be relied upon and should be independently verified with primary sources of information. Taylor and Francis shall not be liable for any losses, actions, claims, proceedings, demands, costs, expenses, damages, and other liabilities whatsoever or howsoever caused arising directly or indirectly in connection with, in relation to or arising out of the use of the Content.

This article may be used for research, teaching, and private study purposes. Any substantial or systematic reproduction, redistribution, reselling, loan, sub-licensing, systematic supply, or distribution in any form to anyone is expressly forbidden. Terms & Conditions of access and use can be found at <http://www.tandfonline.com/page/terms-and-conditions>

## ON A CONTACT PROBLEM OF TWO-LAYER BEAMS COUPLED BY BOUNDARY CONDITIONS IN A TEMPERATURE FIELD

Anton V. Krysko<sup>1</sup>, Jan Awrejcewicz<sup>2</sup>, Igor E. Kutepov<sup>3</sup>, and  
Vadim A. Krysko<sup>3</sup>

<sup>1</sup>*Department of Applied Mathematics and Systems Analysis, Saratov State  
Technical University, Saratov, Russian Federation*

<sup>2</sup>*Department of Automation, Biomechanics and Mechatronics, Lodz University  
of Technology, Lodz and Department of Vehicles, Warsaw University of  
Technology, Warsaw, Poland*

<sup>3</sup>*Department of Mathematics and Modeling, Saratov State Technical University,  
Saratov, Russian Federation*

*We consider a mathematical model of two-layer beams coupled by boundary conditions in a stationary temperature field taking into account geometric nonlinearity. The stationary temperature field is defined by a 2D heat transfer equation with boundary conditions of the first kind. The geometric nonlinearity is introduced via von Kármán's relations for both beams. Equations of beam deflection are derived due to the Euler–Bernoulli hypothesis. The contact interaction is described using Winkler's model. Scenarios of a transition from regular to chaotic regimes are studied. Phase synchronization of beam vibrations versus both character and intensity of the applied temperature field is investigated.*

**Keywords:** Beam; Contact interaction; Temperature

### INTRODUCTION

It is well known that temperature variations have an important influence on a structure dynamics since thermal stresses are generated due to thermal expansion/contraction. It is clear that these effects may change nonlinear dynamics of structural members including straight and curved beams, in particular, when nonlinear vibrations and buckling phenomena are concerned. Since beams are members of various constructions, mechanisms and machines operating in diverse temperature conditions (rocket systems, satellites, engines), the thermodynamic effects play a key role while studying their nonlinear vibrations.

Received 27 May 2014; accepted 23 September 2014.

Address correspondence to J. Awrejcewicz, Department of Automation, Biomechanics and Mechatronics, Lodz University of Technology, 1/15 Stefanowski St., 90-924 Lodz, Poland. E-mail: awrejcew@p.lodz.pl

Color versions of one or more of the figures in the article can be found online at [www.tandfonline.com/uths](http://www.tandfonline.com/uths).

Thermoelastic, geometrically nonlinear vibrations of isotropic, straight and curved beams using the hierarchical finite elements have been studied in [1], where both longitudinal displacements and inertia are taken into account. The temperature variation, thickness and ratio of curvature on the beam regular and chaotic dynamics were illustrated and discussed. It was assumed that the temperature field was not coupled with the beam deformation.

In reference [2] dynamic instability and transient vibrations of a pinned beam with transverse magnetic fields and thermal loads were analyzed. However, the truncated governing equations were strongly reduced to only one linear second-order Mathieu differential equation. The heat phenomenon and primary resonance were illustrated and discussed. Then, a similar study was carried out for physically nonlinear thermoelastic natural pinned beam [3]. The influence of a few control parameters (frequency ratio, load factor, amplitude, damping, temperature increment) on the dynamical stability loss was investigated, but the problem was reduced again to the Mathieu equation, though this time its nonlinear version was studied.

Relatively high temperature variations were applied in thermodynamic analysis for both simply supported and clamped beams assuming that fundamental thermomechanical parameters, like modulus of elasticity, Poisson ratio, linear expansion coefficient and shear modulus are temperature-dependent [4]. Analytical investigations were validated by an experimental analysis.

Thermally pre-stressed laminated and functionally graded beam of variable thickness using the Timoshenko modeling and differential quadrature method was studied from the point of view of its dynamics [5]. It was concluded that both free and forced vibrations of the graded beam were qualitatively similar to the counterpart thermally loaded homogeneous beam with variable thickness.

The out-of-plane free vibration analysis of functionally graded circular curved beam in thermal environment taking into account the first-order shear deformation theory was carried out in reference [6]. Hamilton's principle yielded the governing equations and the associated boundary conditions. The effects of temperature rise, boundary conditions, material and geometrical parameters versus natural frequencies were studied. It was concluded that the temperature-dependent material properties essentially influenced the natural frequencies.

Recently, carbon nanotubes have been applied in nanoelectronics, nanodevices and nanocomposites. Reference [7] addresses a systematic development of the nonlocal Timoshenko beam model to study multi-walled carbon nanotubes exhibiting large-amplitude vibrations in thermal environment. The problem is reduced to a set of coupled nonlinear ordinary differential equations which are solved by the harmonic balance method. In particular, the effects of small-scale parameter, nanotube geometries, temperature variation and the medium elasticity on the dynamics of nanotubes are investigated. Nonlinear vibrations of single-walled carbon nanotubes in an elastic medium via a single-beam model including thermal effects are studied in reference [8]. The amplitude-frequency curves for large-amplitude vibrations were reported. In addition, the influence of thermal variations, boundary conditions, surrounding material constants and variations of geometrical parameters were taken into account.

The multi-layer beams are widely applied in mechatronic systems like sensors of inertial information (they measure circular velocity of an object rotation), in

gyroscopes (micro-electromechanical systems), in micro-cantilever bio-sensors, in optic-mechanical devices, and others. In reference [9] one-, two-, and three-layer beam packages being subjected to the action of a constant and variable current are analyzed. The influence of electromechanical excitation is approximated by a concentrated load in the beam center. It should be emphasized that even for a linear beam model, the system of layers behaves in a nonlinear way due to interaction of the layers and occurrence of the electro-physical quantities.

In work [10] the problem of a simultaneous influence of the temperature field of the first kind boundary conditions and local sinusoidal load on cylindrical shells was presented. In particular, the static load versus temperature intensity of rectangular shells for selected geometric parameters was studied.

A series of bifurcation phenomena was detected, depending on the phase of external periodic excitation. Nonlinear vibrations of continuous systems were investigated in works [11, 12]. In reference [13] the influence of different kinds of the temperature field on the vibration regimes of a one-layer beam was analyzed. It was shown that though a temperature field had a marginal influence on the vibration amplitude, it changed the character of exhibited vibrations. Chaotic zones were decreased with an increase of temperature input. The way in which temperature influenced a scenario of the system transition from regular to chaotic dynamics was also illustrated. The control of system parameters allows researchers to establish a required vibration regime. The latter result makes it possible to keep the system dynamic regime in a safe region, i.e., the mechanical construction may work safely under the action of temperature field and dynamic load.

However, the problem related to investigation of the effects of thermal field on two-layer beam chaotic dynamics and synchronization was not addressed. In particular, our aim was to detect and illustrate the scenarios associated with routes to chaotic vibrations. In addition, the paper discusses a need to develop novel models being close to realistic nonlinear dynamics of continuous systems (here beams), and illustrates novel dynamic phenomena associated with the influence of geometric and design nonlinearity and of the temperature field.

## PROBLEM STATEMENT

We study a two-layer beam, where the layers can contact each other as it is shown in Figure 1. We consider the case when sticking between the layers of the beam is not possible because contact pressure is small.

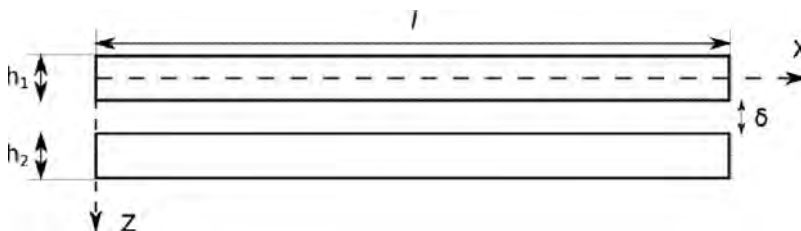


Figure 1 Two-layer beam studied.

The introduced mathematical model is based on the following hypotheses:

1. Any transversal cross section normal to the beam middle curvature remains straight and normal before and after the beam deformation, and the cross section height is unaffected (Euler-Bernoulli hypothesis):

$$\varepsilon_{x,u} = -z \frac{\partial^2 w}{\partial x^2} \tag{1}$$

2. Nonlinear relation between beam deformation and displacement is taken in von Kármán's form:

$$\varepsilon_x = \frac{\partial u}{\partial x} + \frac{1}{2} \left( \frac{\partial w}{\partial x} \right)^2 \tag{2}$$

where:  $u(x, t)$  – middle beam line displacement along the axis  $x$ ;  $w(x, t)$  is beam deflection.

3. Beam material is isotropic, elastic and follows the Duhamel–Neumann rule:

$$\varepsilon_x^z = \varepsilon_x + \varepsilon_{x,i} + \alpha T(x, z) \tag{3}$$

4. Beam temperature is governed by a 2D heat transfer equation, and hence there are not any restrictions on the temperature distribution along the beam thickness; normal stresses occurring on surfaces parallel to the middle beam line are neglected, since they are small in comparison to other stresses. We have applied stationary temperature field. Thermal expansion coefficient ( $\alpha - const$ ) does not depend on temperature, and the beam material is isotropic. Lack of the temperature input ( $T = 0$ ) reduces the problem to a standard one.

The 2D beam space in the rectangular coordinates is as follows:  $\Omega = \{(x, z) \in [0, l] \times [-h_1/2, h_1/2] \wedge [h_1/2 + \delta, h_1/2 + \delta + h_2]\}$ , where:  $l$  is the beam length;  $h_1, h_2$  is the height of the first and second layer, respectively;  $\delta$ – stands for the clearance magnitude.

Equations governing dynamics of the beam layers embedded in the temperature field have the following form:

$$\frac{1}{\lambda^2} \left\{ L_1(w_k, u_k) + L_2(w_k, w_k) - \frac{1}{12} \frac{\partial^4 w_k}{\partial x^4} \right\} - \frac{\partial}{\partial x} \left( \frac{\partial w_k}{\partial x} N_x^{Tk} \right) - \frac{\partial^2 M_x^{Tk}}{\partial x^2} \tag{4}$$

$$- \frac{\partial^2 w_k}{\partial t^2} - \varepsilon \frac{\partial w_k}{\partial t} + q - q_k = 0$$

$$\frac{\partial^2 u_k}{\partial x^2} + L_3(w_k, w_k) - \frac{\partial N_x^{Tk}}{\partial x} - \frac{\partial^2 u_k}{\partial t^2} = 0, k = 1, 2 \tag{5}$$

where  $L_1(w_k, u_k) = \frac{\partial^2 u_k}{\partial x^2} \frac{\partial w_k}{\partial x} + \frac{\partial^2 w_k}{\partial x^2} \frac{\partial u_k}{\partial x}$ ;  $L_2(w_k, w_k) = \frac{3}{2} \frac{\partial^2 w_k}{\partial x^2} \left( \frac{\partial w_k}{\partial x} \right)^2$ ;  $L_3(w_k, w_k) = \frac{\partial^2 w_k}{\partial x^2} \frac{\partial w_k}{\partial x}$ ;  $q_k = K(w_1 - \delta - w_2) \Psi$ ;  $\Psi = 1 + \text{sign}(w_1 - w_2)$ ;  $w_k$  is the displacement along axis  $z$ ;  $u_k$  is the displacement along axis  $x$ ;  $N^{Tk}$  stand for the temperature longitudinal stress;  $M^{Tk}$  is the temperature bending moment;  $q$  represents the

transversal load;  $t$  is the time;  $\varepsilon$  is the damping coefficient characterizing the dissipative properties of the beam environment.;  $K$  is the Winkler-type stiffness;  $q_k$  represents the contact pressure;  $\lambda$  is the non-dimensional coefficient.

The main idea of studying the considered contact Problems of beams embedded into a temperature field and taking into account beam geometric non-linearities relies on solution of Eqs. (4)–(5) assuming an explicitly defined coupling of the contact pressure  $q_k$  with the deflections  $w_k$  of the beam center line. This approach removes a need of the Green function construction on each of the iterational step, which is widely used while solving the contact problems in a classical way. It should be emphasized that it is impossible to describe the Green functions analytically, and also their numerical estimations belongs rather to difficult tasks. Here, the contact pressure is removed from the number of unknown functions, and it is a continuous function achieving zeroth value on boundaries of the contact zones. At each time step we construct on iterative process of finding a solution of the non-linear differential equations, which is appropriately matched with the process of improvement of the contact area estimation.

The given governing equations have a non-dimensional form, whereas the transformation between dimensional and non-dimensional quantities are as follows:

$$\begin{aligned} \bar{w}_k &= \frac{w_k}{h_k}, \quad \bar{u}_i = \frac{u_k l}{h_k^2}, \quad \bar{x} = \frac{x}{l}, \quad \lambda = \frac{l}{h_k}, \quad \bar{q} = q \frac{l^4}{h_k^4 E}, \quad \bar{t} = \frac{t}{\tau}, \quad \tau = \frac{l}{c}, \quad c = \sqrt{\frac{Eg}{\gamma}} \\ \bar{\varepsilon} &= \frac{\varepsilon l}{c}, \quad \bar{N}_x^{Tk} = \frac{N_x^{Tk} l^2}{E h_k^3}, \quad \bar{M}_x^{Tk} = \frac{M_x^{Tk} l}{E h_k^2}, \quad \bar{T}_k = \alpha T_k \lambda^2 \end{aligned} \quad (6)$$

In the following, the symbol ( $\bar{\quad}$ ) is omitted for the sake of simplicity.

Governing equations require boundary conditions (BC). As an example we take (7), which corresponds to simple support and clamping of the beam ends:

$$w_k(0, t) = w_k(l, t) = u_k(0, t) = u_k(l, t) = w'_{kx}(0, t) = M_{kx}(l, t) = 0 \quad (7)$$

and the following initial conditions are taken

$$w(x, 0) = \dot{w}(x, 0) = u(x, 0) = \dot{u}(x, 0) = 0 \quad (8)$$

Temperature field is defined for each beam layer via Eq. (9) with the first kind boundary conditions (10):

$$\frac{\partial^2 T_k}{\partial x^2} + \frac{1}{\lambda^2} \frac{\partial^2 T_k}{\partial z^2} = 0 \quad (9)$$

$$T_k(x_0, z) = f_{1,k}(z), \quad T_k(x_l, z) = f_{2,k}(z), \quad T_k(x, z_0) = f_{3,k}(x), \quad T_k(x, z_l) = f_{4,k}(x) \quad (10)$$

To reduce PDEs to ODEs we apply FDM and Taylor series expansion in the vicinity of point  $x_i$ . We take into account the mesh  $G_N = \{0 = x_i = 1, \quad x_i = i/N, \quad i = 0, \dots, N\}$ .

PDEs (4), (5) are reduced to the second-order ODEs (11) using the difference operators. In each mesh point  $0, \dots, n$ , where  $n$  is the spatial co-ordinate partitions number, we take finite differences and construct finite difference operators  $\Lambda_x(\cdot)$ ,  $\Lambda_{x^2}(\cdot)$ ,  $\Lambda_{x^4}(\cdot)$  for approximation of the order  $O(\Delta^2)$ , where  $\Delta$  is the mesh step:

$$\left\{ \begin{aligned} \ddot{u}_i^k &= \Lambda_{x^2}(u_i^k) + \Lambda_x(w_i^k) \Lambda_{x^2}(w_i^k) - \Lambda_x(N_i^{T_k}) \\ \ddot{w}_i^k + \varepsilon \dot{w}_i^k &= \lambda^2 \left( -\frac{1}{12} \Lambda_{x^4}(w_i^k) + \Lambda_{x^2}(u_i^k) \Lambda_x(w_i^k) + \Lambda_{x^2}(w_i^k) \Lambda_x(u_i^k) \right) \\ &+ \frac{3}{2} (\Lambda_x(w_i^k))^2 \Lambda_{x^2}(w_i^k) - \Lambda_{x^2}(w_i^k) N_i^{T_k} + \Lambda_x(w_i^k) \Lambda_x(N_i^{T_k}) - \Lambda_{x^2}(M_i^{T_k}) + q \\ &+ K(w_i^1 - \delta - w_i^2) \Psi, \quad k = 1, 2 \end{aligned} \right. \quad (11)$$

Temperature terms occurring in (11) are computed with respect to the boundary conditions of the heat transfer equation. The obtained second-order ODEs are reduced to the first-order ODEs, and then they are solved using the fourth-order Runge–Kutta method. Note that the boundary conditions require also a transformation to finite differences.

**RELIABILITY OF THE RESULTS**

To study beam vibration regimes the following control parameters were investigated (see Table 1). The temperature field is stationary and its intensity is chosen in a way to keep constant the physical material characteristics.

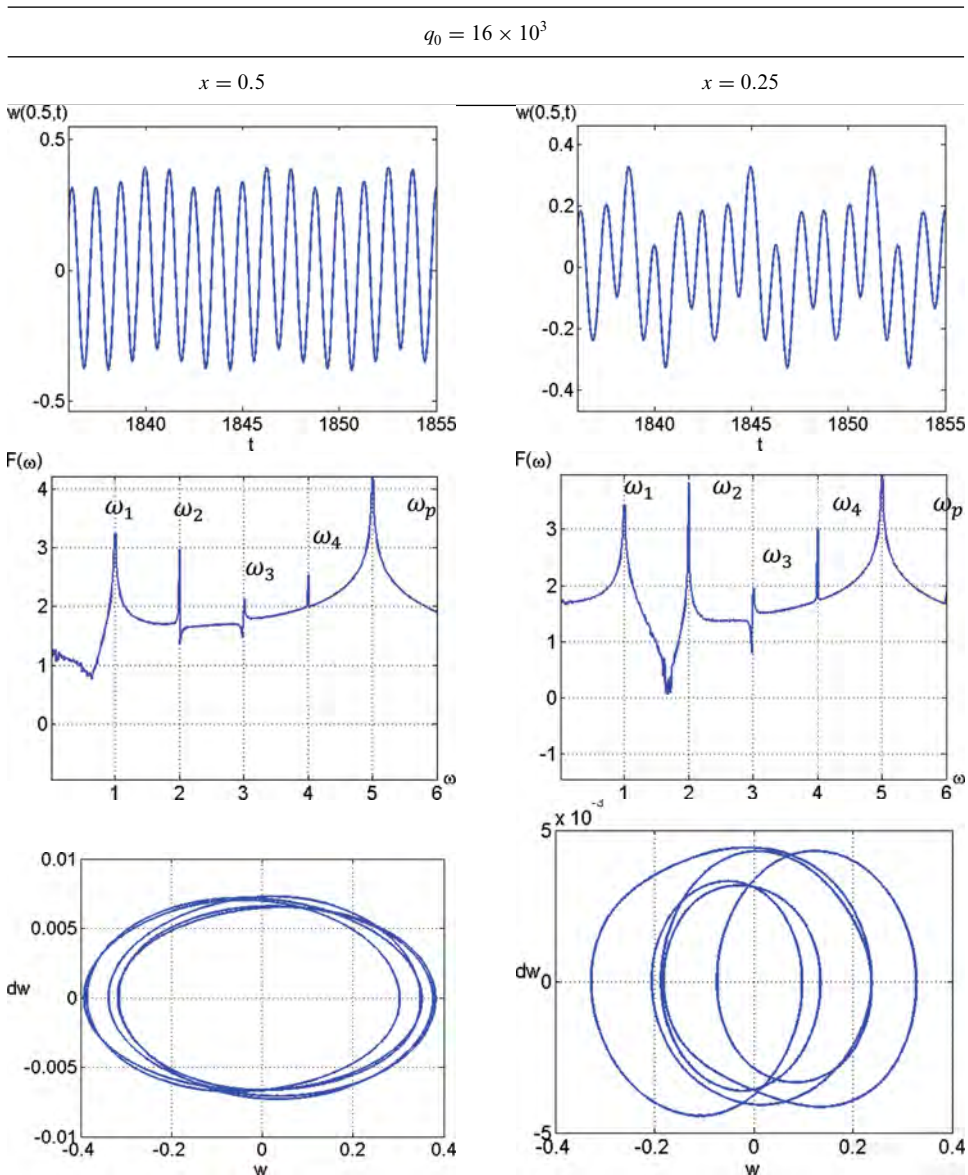
Transversal load acts in the  $z$  axis direction and is governed by the equation  $q = q_0 \sin(\omega_p t)$ , where:  $q_0$  is the load,  $\omega_p$  means the excitation frequency,  $t$  represents the time. The number of mesh nodes  $n$  is implied by the investigation of convergence of the results while applying different numerical approaches. The clearance was set  $\delta = 1000$  to implement the lack of contact interaction. All investigations were carried out for the central point of the beam. It well represents the vibration regimes of other beam points. Table 2 gives a comparison between analytical data for the upper beam for  $T_k = 0$  for  $x = 0.5$ , and for  $x = 0.25$  on the basis of a signal (time history), the Fourier power spectrum and phase portrait.

It follows from Table 2 that in the Fourier spectrum for  $x = 0.5$  and  $x = 0.25$  we have the same frequency set:  $\omega_1 = 1/5\omega_p = 1$ ,  $\omega_2 = 2/5\omega_p = 2$ ,  $\omega_3 = 3/5\omega_p = 3$ ,  $\omega_4 = 4/5\omega_p = 4$ . Phase portraits exhibit 5 stable orbits.

**Table 1** The values of fixed parameters

Parameter	Value
$n$	80
$\omega_p$	5
$T_k$	0; 200; 300
$t$	1836.2348
$\Delta t$	1/256
$q_0$	$1 \times 10^3 \dots 50 \times 10^3$
$\varepsilon$	1
$\lambda$	50

**Table 2** Time histories, frequency power spectra and phase portraits of two beam points ( $x = 0.5$ ;  $x = 0.25$ )



To investigate convergence of the solution we applied the parameters given in Table 3. We took into account the vibration harmonic ( $q_0 = 500$ ) and chaotic ( $q_0 = 60 \times 10^3$ ) regimes.

In the case of a periodic regime an increase of nodes number does not yield any qualitative changes. Only small changes of the signal amplitudes are observed at the amount of 1–2%. In the Fourier power spectrum there is one frequency



**Table 3** Time history, power spectra and Poincaré maps versus beam partitions  $n$  for  $q_0 = 500$  and  $q_0 = 60000$

n	Signal	Power spectrum	Poincaré map
$q_0 = 500$			
60			
80			
100			
$q_0 = 60 \times 10^3$			
60			
80			
100			

$\omega_p = 5$  for all applied variants, which is confirmed by one point on the Poincaré map. However, though for  $q_0 = 60 \times 10^3$  we have essential changes regarding both form and amplitude of the signal, but till  $n = 90$  a convergence regarding Fourier spectrum and Poincaré map is observed.

Because a further increase of the mesh nodes yields changes of the Poincaré map, a threshold of errors magnitude introduced by the applied numerical methods appears. It should be mentioned that a further increase of the nodes yields the occurrence of new frequencies which are not exhibited by a smaller number of selected nodes. In other words, it means that the choice of  $n = 80$  is validated.

## ANALYSIS OF VIBRATIONS

We take the control parameters from Table 1 and we study the obtained data via signals, Fourier power spectra, amplitude characteristics in time-space coordinates for a set of  $q_0$  values. The scheme shown in Figure 2 gives a graphic interpretation of the temperature influence on the beam. Boundary conditions for the heat transfer equation, where  $T_k(x, z)$  is the function governing temperature distribution along a beam, has the following form:

$$\begin{cases} T_1(x, -h/2) = 0 \\ T_1(x, h/2) = 0 \\ T_1(0, z) = 0 \\ T_1(1, z) = 0 \end{cases} \quad \begin{cases} T_2(x, -h/2) = 0 \\ T_2(x, h/2) = 0 \\ T_2(0, z) = 0 \\ T_2(1, z) = 0 \end{cases} \quad (12)$$

Let us begin the analysis with the data reported in Table 4 obtained for the lack of temperature field  $T_k = 0$ .

Range of  $q_0 \leq 3 \times 10^3$  (not shown) corresponds to the lack of contact between the beams, i.e. the value of the first beam deflection  $w_1$  does not overcome the value of 0.1 being equal to the beam clearance. The first beam vibrates periodically, whereas the second exhibits a contact lack with the first beam. The Fourier power spectrum shows only the frequency of excitation  $\omega_p = 5$  and periodic vibrations of the upper beam. Amplitude-time characteristics and phase portraits are in agreement with the power spectrum.

When the excitation amplitude  $q_0$  achieves the value of  $4 \times 10^3$ , the bottom beam vibrates, i.e., a contact between beams is observed. The frequency power spectrum contains the independent frequency  $\omega_1 = 1.9$ , and the bottom beam, in spite of the noisy frequencies, is characterized by the same frequencies as the upper beam is, i.e.,  $\omega_p = 5$  and  $\omega_1 = 1.9$ . Observe that the amplitude-time surface of the bottom beam is different from a plane surface.



Figure 2 Scheme of beam two-layers and the temperature action ( $T = 0$ ).

**Table 4** Beam vibration characteristics for different  $q_0$

$q_0$	Time history	Power spectrum (upper beam)	Power spectrum (bottom beam)	Shell spatiotemporal deflection	Phase portrait (upper beam)
$5 \times 10^3$					
$15 \times 10^3$					
$40 \times 10^3$					
$50 \times 10^3$					

An increase to the external load up to  $q_0 = 5 \times 10^3$  already exhibits three frequencies,  $\omega_p = 5$ ,  $\omega_1 = 1.9$  and  $\omega_2 = 1.1$ . A further increase of  $q_0$  up to  $10 \times 10^3$  (not shown) implies the occurrence of a number of vibration frequencies of the upper beam. Namely, the frequencies  $\omega_4 = 2.7$  and  $\omega_3 = 4.2$  appear. The following linear relations between the frequencies appear:  $\omega_1 = \omega_2 + 0.16\omega_p$ ,  $\omega_4 = \omega_1 + 0.16\omega_p$ , and  $\omega_3 = \omega_4 + \omega_1$ . Phase trajectories of the upper beam begin to diverge remarkably.

It is interesting to note that a further increase of the loading values for the upper beam yields more disordered vibrations, whereas vibrations of the bottom beam become more ordered. For  $q_0 = 25 \times 10^3$  (not shown) peaks of the frequency spectra of the upper and bottom beams coincide in full. The distribution of frequencies is governed by the series  $\omega_n = n \times 1/5\omega_p$ , where  $n = 1, \dots, 5$ .

A further increase of the load implies a noisy spectrum in the zone of small vibrations, which manifests an increase of frequency of the contacts between beams. Phase portraits indicate a change of the vibrational regime. Amplitude-time characteristics of the beam deflection also indicates irregularity of the upper beam vibrations.

For  $q_0 = 50 \times 10^3$  on the frequency spectrum of both beams, a series of coupled frequencies  $\omega_n = n \times \frac{1}{10\omega_p}$ , where  $n = 1, \dots, 10$ , is observed. The time history of the upper beams exhibits chaotic dynamics, which is also demonstrated by the phase portrait. Amplitude-frequency characteristics also imply the occurrence of the chaotic regime in both temporal and spatial domains.

Next, we study the data obtained for the same kind of temperature excitation, subjected to both beam ends, with the same intensity, as it is shown in the scheme presented in Figure 3. The boundary conditions for the heat transfer equations have the following form:

$$\begin{cases} T_1(x, -h/2) = 200 \\ T_1(x, h/2) = 0 \\ T_1(0, z) = 0 \\ T_1(1, z) = 0 \end{cases} \quad \begin{cases} T_2(x, -h/2) = 200 \\ T_2(x, h/2) = 0 \\ T_2(0, z) = 0 \\ T_2(1, z) = 0 \end{cases} \quad (13)$$

Let us analyze the data (Table 5) obtained for temperature  $T = 200^\circ\text{C}$  on one side of each beam. Already for small values of the external load amplitude  $q_0 = 1 \times 10^3$  (not shown), a contact interaction between beams occurs implied by the temperature action. The frequency power spectra for both beams, in spite of a small noise generated by the contact, exhibits only one frequency  $\omega_p = 5$ .

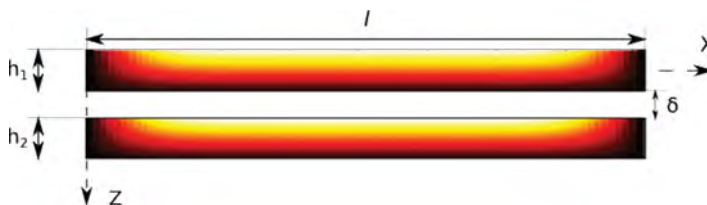
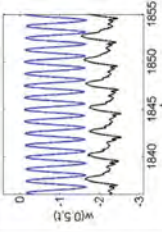
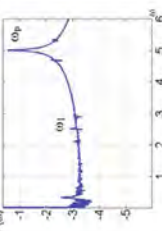
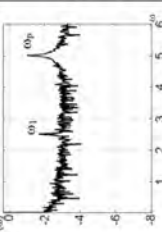
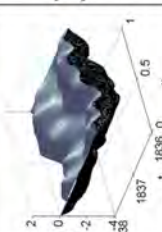

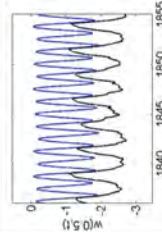
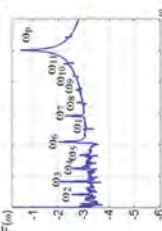
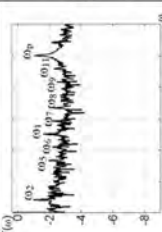

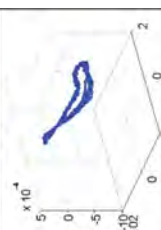
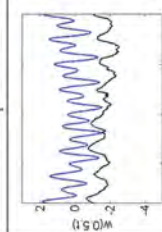
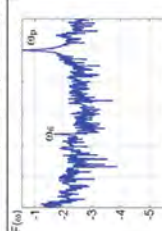
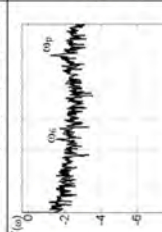
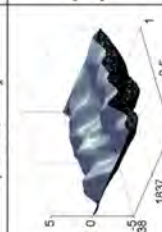
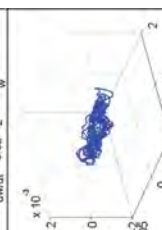
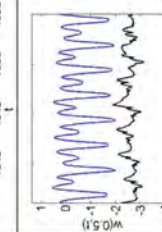
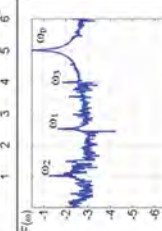
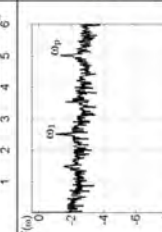
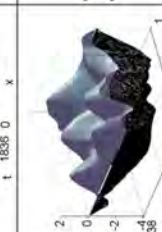
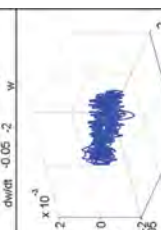


Figure 3 Scheme of beam two-layers and temperature excitation (two layers are heated).

**Table 5** Beam vibration characteristics for different  $q_0$

$q_0$	Time history	Power spectrum (upper beam)	Power spectrum (bottom beam)	Shell spatiotemporal deflection	Phase portrait (upper beam)
$30 \times 10^3$					
$35 \times 10^3$					
$45 \times 10^3$					
$50 \times 10^3$					

Increasing  $q_0$  up to  $4 \times 10^3$  (not shown) does not change the dynamics qualitatively, since only a small increase of the amplitudes of vibrating beams is observed. For  $q_0 = 5 \times 10^3$  the frequency power spectrum of both beams exhibits the frequency  $\omega_1 = 1/2\omega_p = 2.5$ . An increase of the external load up to  $q_0 = 10 \times 10^3$  (not shown) causes that  $\omega_1$  vanishes from the upper beam spectrum, but it is preserved on the bottom beam power spectrum.

A further increase of the external load does not change essentially the beam vibrations regime. The frequency power spectrum, time history and phase portrait show subharmonic vibrations of the upper beam. However, beginning from  $q_0 = 35 \times 10^3$  a sudden change of the vibrational regime takes place. In the frequency power spectrum there is a set of linearly dependent frequencies governed by the equation  $\omega_n = n \times 1/10\omega_p$ , where  $n = 1, \dots, 10$ . Phase trajectories again present the orbital character, though slightly deformed. For  $q_0 = 45 \times 10^3$  the frequencies of the upper beam as well as the phase portraits become noisy, which approves the occurrence of chaos.

A further increase of the load implies an increase of the spatio-temporal chaos, which is also exhibited by the temporal-spatial characteristics. It should be noticed in power spectra of both beams that the relation between frequencies differs from that without the temperature influence. In the case of the upper beam we have:  $\omega_1 = 1/2\omega_p = 2.5$ ,  $\omega_2 = 1/5\omega_p = 1$  and  $\omega_3 = 4/5\omega_p = 4$ , whereas in the case of the bottom beam we have  $\omega_p = \omega_3 + \omega_2$  and  $\omega_1 = 1/2\omega_p = 2.5$ .

We investigate further scenarios of the beam vibration regimes, when the temperature field applies only to the upper beam (Figure 4). For this type of the temperature influence the thermal boundary conditions take the following form:

$$\begin{cases} T_1(x, -h/2) = 200 \\ T_1(x, h/2) = 0 \\ T_1(0, z) = 0 \\ T_1(1, z) = 0 \end{cases} \quad \begin{cases} T_2(x, -h/2) = 0 \\ T_2(x, h/2) = 0 \\ T_2(0, z) = 0 \\ T_2(1, z) = 0 \end{cases} \quad (14)$$

Taking into account the data reported in Table 6, the following scenarios of the beam vibrations from regular to chaotic are detected. For  $q_0 = 1 \times 10^3$  (not shown) the Fourier frequency spectrum associated with the upper beam exhibits only one frequency  $\omega_p = 5$ , just like the noisy components caused by beam contact interactions. Temperature influences strongly the vibration forms, which is monitored via observation of the amplitude characteristic in the space-time coordinates. A further increase of parameter  $q_0$  up to the value  $25 \times 10^3$  does not introduce any qualitative change of the vibration regime, i.e. the subharmonic regime is observed.

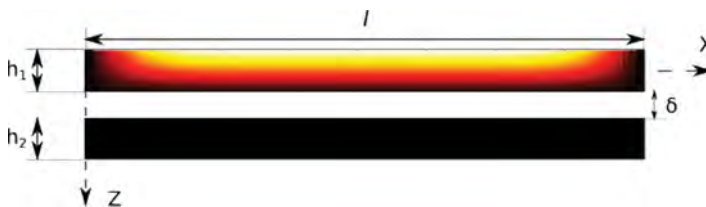


Figure 4 Scheme of beam two-layers and temperature action (the first layer is heated from the top).

**Table 6** Beam vibration characteristics for different  $q_0$

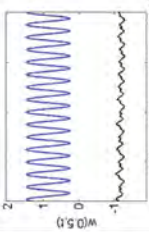

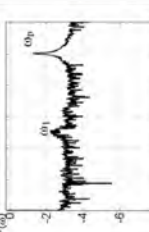


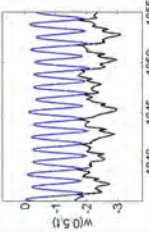
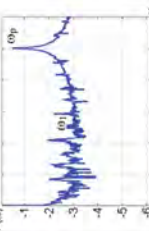
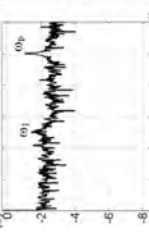
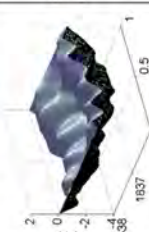

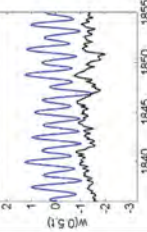
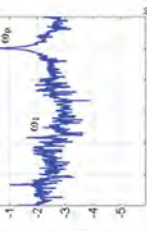

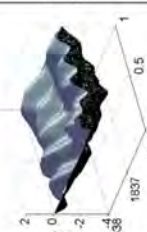

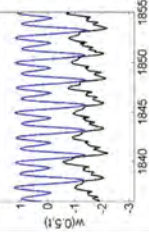
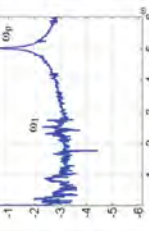
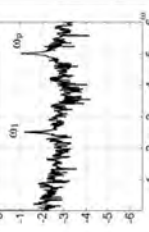
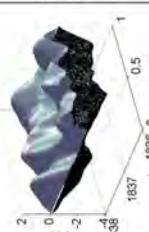
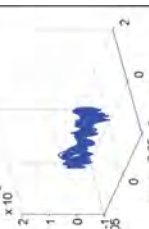





	Time history	Power spectrum (upper beam)	Power spectrum (bottom beam)	Shell spatiotemporal deflection	Phase portrait (upper beam)
$0b$					
$25 \times 10^3$					
$35 \times 10^3$					
$40 \times 10^3$					
$50 \times 10^3$					

Table 7 Beam vibration characteristics for different  $q_0$

$q_0$	Time history	Power spectrum (upper beam)	Power spectrum (bottom beam)	Shell spatiotemporal deflection	Phase portrait (upper beam)
$25 \times 10^3$					
$35 \times 10^3$					
$40 \times 10^3$					
$50 \times 10^3$					



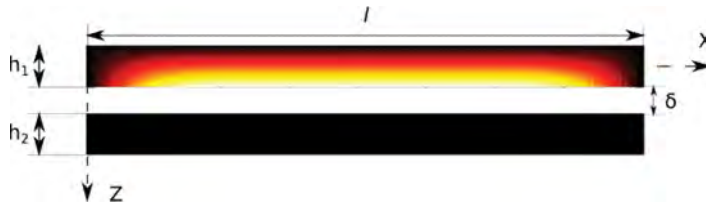


Figure 5 Scheme of beam two-layers and temperature excitation (the first layer is heated from below).

For  $q_0 = 25 \times 10^3$  both beam layers exhibit a novel frequency  $\omega_1 = 1/2\omega_p = 2.5$ . Vibrations take a more complex form which is presented by the deformed phase orbits. Increasing the excitation amplitude up to  $q_0 = 30 \times 10^3$  (not shown) implies the frequency power spectrum reconstruction, and the new frequencies series appears for the upper beam, whereas the bottom beam vibration regime remains unchanged. Phase trajectories exhibit chaotic dynamics.

At a further increase of  $q_0$  up to  $40 \times 10^3$ , the upper beam again shows  $\omega_1 = 1/2\omega_p = 2.5$ . The series of dependent frequencies and the character of vibrations is more complex. For  $q_0 = 50 \times 10^3$  our investigated mechanical system is in the deep chaotic state.

We also investigated the case when the following non-symmetric temperature boundary conditions are applied (see Figure 5):

$$\begin{cases} T_1(x, -h/2) = 0 \\ T_1(x, h/2) = 200 \\ T_1(0, z) = 0 \\ T_1(1, z) = 0 \end{cases} \quad \begin{cases} T_2(x, -h/2) = 0 \\ T_2(x, h/2) = 0 \\ T_2(0, z) = 0 \\ T_2(1, z) = 0 \end{cases} \quad (15)$$

This case is different from the previously studied, since the change of the temperature field does not change the vibration regimes for the properly chosen control parameters. Similarity of the regimes reported in Tables 6 and 7 for all values of the control parameter  $q_0$  should be emphasized. A negligible change of the time history of the bottom beam is yielded by the beam change caused by the initial beam bending due to the temperature action. Our mechanical system approaches chaos via period doubling bifurcations. Frequency power spectra of both beams exhibit the frequencies  $\omega_p = 5$  and  $\omega_1 = 1/2\omega_p = 2.5$ .

## CONCLUSIONS

We have proposed a mathematical model of flexible elastic beams coupled via the boundary conditions and embedded into a temperature field, when the upper beam layer is transversally harmonically excited. Analysis of the dynamics of two-layer beams is carried out and novel scenarios of routes from regular to chaotic dynamics versus control parameters are illustrated and discussed. In particular, strong sensitivity of the investigated system versus both type and intensity of the thermal excitation is reported. Furthermore, it is shown that a symmetric change of the thermal boundary conditions does not have a qualitative influence on the beam vibrational regime.

## FUNDING

This paper was financially supported by the National Science Centre of Poland under the grant MAESTRO 2, No. 2012/04/A/ST8/00738, for the years 2013–2016.

## REFERENCES

1. P. Ribeiro and E. Manoach, The Effect of Temperature on the Large Amplitude Vibrations of Curved Beams, *Journal of Sound and Vibration*, vol. 285, pp. 1093–1107, 2005.
2. G.-Y. Wu, The Analysis of Dynamic Instability and Vibration Motions of a Pinned Beam with Transverse Magnetic Fields and Thermal Loads, *Journal of Sound and Vibration*, vol. 284, pp. 343–360, 2005.
3. G.-Y. Wu, The Analysis of Dynamic Instability on the Large Amplitude Vibrations of a Beam with Transverse Magnetic Fields and Thermal Loads, *Journal of Sound and Vibration*, vol. 302, pp. 167–177, 2007.
4. J. Avsec and M. Oblak, Thermal Vibrational Analysis for Simply Supported Beam and Clamped Beam, *Journal of Sound and Vibration*, vol. 308, pp. 514–525, 2007.
5. H. J. Xiang and J. Yang, Free and Forced Vibration of a Laminated FGM Timoshenko Beam of Variable Thickness Under Heat Conduction, *Composites: Part B*, vol. 39, pp. 292–303, 2008.
6. P. Malekzadeh, M.R. Golbahar Haghighi, and M.M. Atashi, Out-of-Plane Free Vibration of Functionally Graded Circular Curved Beams in Thermal Environment, *Composite Structures*, vol. 92, pp. 541–552, 2010.
7. R. Ansari and H. Ramezannezhad, Nonlocal Timoshenko Beam Model for the Large-Amplitude Vibrations of Embedded Multiwalled Carbon Nanotubes Including Thermal Effects, *Physica E*, vol. 43, pp. 1171–1178, 2011.
8. R. Ansari, M. Hammatnezhad, and J. Rezapour, The Thermal Effect on Nonlinear Oscillations of Carbon Nanotubes with Arbitrary Boundary Conditions. *Current Applied Physics*, vol. 11, pp. 692–697, 2011.
9. S. Gutschmidt and O. Gottlieb, Bifurcations and Loss of Orbital Stability in Nonlinear Viscoelastic Beam Arrays Subject to Parametric Actuation, *Journal of Sound and Vibration*, vol. 329, pp. 3835–3855, 2010.
10. A. V. Krysko, J. Awrejcewicz, E. S. Kuznetsova, and V. A. Krysko, Chaotic Vibrations of Closed Cylindrical Shells in a Temperature Field, *International Journal of Bifurcation and Chaos*, vol. 18, No. 5, pp. 1515–1529, 2008.
11. J. Awrejcewicz, V.A. Krysko, *Chaos in Structural Mechanics*, Springer, Berlin, 2008.
12. J. Awrejcewicz, V. Krysko, I. Papkova, and A. Krysko, Routes to Chaos in Continuous Mechanical Systems, *Chaos, Solitons & Fractals*, vol.4, pp. 45, 2012.
13. V. A. Krysko, J. Awrejcewicz, I. E. Kutevov, N. A. Zagniboroda, I. V. Papkova, A. V. Serebryakov, and A. V. Krysko, Chaotic Dynamics of Flexible Beams with Piezoelectric and Temperature Phenomena, *Physics Letters A*, vol. 377, pp. 2058–2061, 2013.